



# The Design and Construction of a Vertical Wind Tunnel for the Study of Untethered Firebrands in Flight

*I.K. Knight, CSIRO Forestry and Forest Products, PO Box E4008,  
Kingston ACT 2604, Australia, e-mail: Ian.Knight@ffp.csiro.au*

**Abstract.** The design and construction of a wind tunnel with a vertical working section, which was used successfully for the study of untethered firebrands at their terminal velocity, is described. Two unique features in this tunnel design set it aside from previous vertical wind tunnels: the vertical working section has a divergent taper that allows a firebrand to find its terminal velocity within a velocity gradient, and the velocity of the boundary layer of the working section has been forced to a higher speed than the central zone to stop the firebrand impacting on the working section walls. These features in combination with a responsive speed control on the fan allow observation of burning firebrands throughout their viable lifetime in freefall with changing terminal velocities. This paper is intended as a synthesis of wind tunnel design and as a guide to researchers considering building similar devices to study the untethered flight characteristics of local species of firebrands.

**Key words:** vertical wind tunnel, tapered working section, wind tunnel design, untethered firebrands, spotting process, spotfire research

## 1. Background

In January 1994 wildfires caused much destruction throughout New South Wales, Australia. In the city of Sydney, fires in green reserves within the built-up area caused considerable problems for suppression through the formation of small spotfires ahead of the main front. These spotfires developed as individual fires and enabled the wildfires to jump breaks in topography and, in some cases, even rivers, and caused the majority of damage when they burnt into adjacent suburbs.

The process of spotfire formation or spotting, where embers from the fire front are lofted high in the convection column, transported downwind, and deposited ahead of the main front, is widely acknowledged as the main factor that limits fire suppression and enables fire to spread across broken topography. The actual study of this process has been limited due to the complex nature of the problem—even the source of firebrands is not fully understood as there are a limited number of direct observations (although in most cases it is presumed that loose bark comprises the majority of firebrands).

Tarifa *et al.* [1] investigated the burning and flight characteristics of tethered samples of wood in both horizontal and vertical wind tunnels. Tarifa *et al.* [2] expanded the study using a vertical wind tunnel with a tapered working section and an untethered wooden sample to verify the results found with tethered samples. All three wind tunnel designs

utilised a suction blower placed at the end of the tunnel and there was no attempt at air flow uniformity apart from a bell mouth entry to the tunnel. Tarifa *et al.* [2] found that the vertical tapered working section produced a high degree of vorticity that appeared to induce a strong tumbling motion in the samples which could not be removed even with several modifications.

Muraszew *et al.* [3, 4] also investigated tethered firebrand samples in a wind tunnel but give no details on the design of the tunnel, except that it was a horizontal tunnel with controlled air temperature and humidity. Following the hypothesis that firebrands could only be lofted great distances in fire whirls, Muraszew *et al.* [3] also constructed a vertical fire whirl generator to investigate ignition and burning characteristics of firebrand samples in fire whirls.

In order to properly investigate the flight and burning characteristics of species of bark commonly thought to be the major cause of spotting, the ability to loft an untethered sample on a well-manipulated cushion of air was required. A wind tunnel with a vertical tapered working section was built by the Bushfire Behaviour and Management Group of the Commonwealth Scientific and Industrial Research Organisation (CSIRO) Division of Forestry and Forest Products. The tapered working section enabled the firebrand sample to settle at a quasi-stationary level matching its evolving terminal velocity as it burnt.

The tunnel was used successfully in a study of the aerodynamic and burning characteristics of bark from the notorious Australian stringybark tree *Eucalyptus obliqua* [5] (Figure 1). Burning bark from this species were found to have a typical initial terminal velocity of  $3\text{--}5\text{ m s}^{-1}$  and could remain flaming for in excess of 500 s.

At its maximum velocity, the tunnel has been shown to be capable of lofting cones ( $\approx 235\text{ g}$ ) from *Pinus pinea*, the predominant species in the vicinity of the wind tunnel. The tunnel could be used to investigate the aerodynamic and combustion characteristics of a large variety of materials.



**Figure 1. Photo of burning *Eucalyptus obliqua* bark at terminal velocity in the CSIRO vertical wind tunnel.**

## 2. Wind Tunnel Principles

All modern wind tunnels that produce a highly uniform flow of air operate on the same fundamental design principles. Highly turbulent air from the fan is slowed in a widening duct called the *diffuser*. The velocity extremes produced as a result of the turbulent air flow are moderated by screens inserted in the diffuser section. The screens must have adequate resistance to produce an even air flow but not result in a pressure drop which would prevent the fan from delivering the required air flow. The air is then passed through a *straightening section*—a honeycomb-like array of short, small diameter tubes. Each tube in the straightening section is aligned in the streamwise direction. This acts to straighten the flow by removing large diameter eddies.

This air, now moving slowly, and fairly uniformly, within the widest cross section of the tunnel, then passes to the *contractor*. The contractor constricts the airflow forcing the air to accelerate. Energy is added equally to each parcel of air. Variations in energy (mean or turbulent) of the ingoing airstream remain as an insignificant component of the accelerated flow at the outlet. The degree of curvature of the contractor walls is critical; any separation of the flow from the contractor walls will produce large unwanted eddies. The uniform accelerated airflow passes into the *working section* where the aerodynamic studies are performed.

As bends in the tunnel produce turbulence and unwanted vortices, wind tunnels generally have the critical components upstream of the working section (i.e. diffuser and contractor) on the one axis. However, as the CSIRO design criteria called for a vertical working section and there were height limitations in the local government building and design specification, a *turning section* was needed to minimise height by separating fan and diffuser sections from contractor and working sections.

## 3. Design and Construction of the CSIRO Vertical Wind Tunnel

### 3.1. General

The CSIRO vertical wind tunnel was fabricated in sections and assembled on site. Tunnel walls are mostly constructed from 12 mm thick plywood. The tunnel is housed in a scaffold framed structure clad in corrugated iron. A full description of the construction of the CSIRO vertical wind tunnel is given by Knight *et al.* [6].

### 3.2. The Fan

The fan selected to power the wind tunnel was a size 44 single-width single-inlet backward-inclined centrifugal blower [7]. It delivers  $11 \text{ m}^3 \text{ s}^{-1}$  at a pressure of 650 pascals. Our calculations—which will be summarised later—called for a capability of delivering this volume at 300 pascals. Blowers of this size and their matching speed controllers are readily available as they are designed and built for rugged use in the air-conditioning industry.

### 3.3. The Diffuser

The highly turbulent air flow from the fan exit is slowed and evened out in the diffuser section. The wall contours are not critical and the widening of the flow can occur quite

rapidly. In our diffuser, the fan exit dimensions of 1100 mm × 900 mm are widened to 2000 mm × 2000 mm over a distance of 4.8 metres.

### 3.4. The Screens

Two screens of perforated sheet metal were used as a cheap alternative to the traditional heavy-duty woven gauze. The positions of the screens in the diffuser are shown in Figure 2. Screen #1 is 1346 mm × 1206 mm, and has a hole diameter of 7.94 mm,

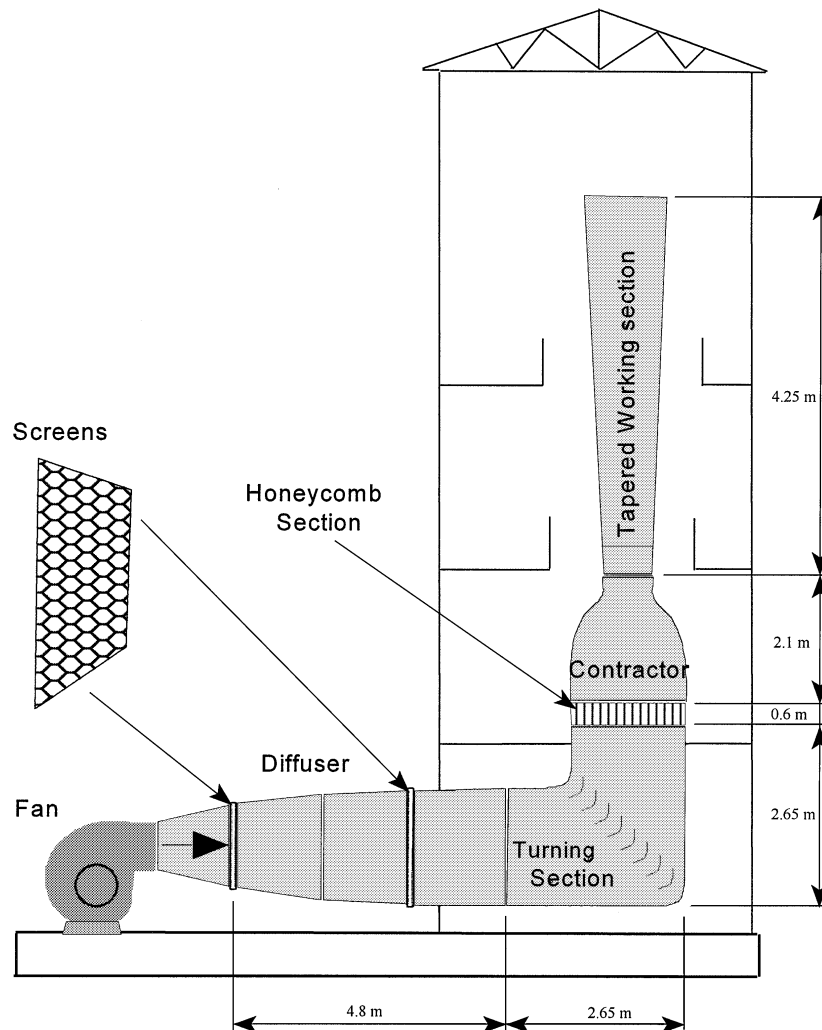


**Figure 2. The general layout and components of the CSIRO vertical working section wind tunnel. The tunnel is housed in a clad scaffolding that provides protection and safe access to the working section.**

spaced to give an open ratio,  $b$ , of 62%. Screen #2 is 1956 mm  $\times$  1956 mm, and has a hole diameter of 4.76 mm and an open ratio of 51%. Using the formula for the coefficient of resistance,  $k$ , described by Mentah [8]:

$$k = \frac{1 - b}{b^2} \quad (3.1)$$

each screen was calculated to have a coefficient of resistance of 0.989 and 1.884 respectively.

The pressure drop across each screen is given by:

$$\Delta P = \frac{1}{2} \rho k v^2 \quad (3.2)$$

where  $\Delta P$  in Pa is the change in pressure,  $\rho$  is the density of air (1.27 kg m<sup>-3</sup>),  $k$  is the coefficient of resistance for the screen and  $v$  (m s<sup>-1</sup>) is the velocity of air passing through the screen. The pressure drop calculated for an air volume flow of, for example, 10 m<sup>3</sup> s<sup>-1</sup> is 22.9 Pa for screen #1 and 7.8 Pa for screen #2.

### 3.5. Turning Section

The purpose of the turning section is to turn the air through 90 degrees without introducing large scale turbulence or loss of uniformity of airflow. The right-angled turning section consists of a metal corner section that houses the turning vanes. This section is mounted between two plywood modules using pinewood flanges.

The turning section contains 20 turning vanes. Each 90° turning vane has a radius of curvature of 353.5 mm, a chord length of 500 mm and an arc length of 555.3 mm. The turning vanes were constructed from light gauge sheet metal. To maintain rigidity the vanes were constructed as two separate modules located side by side such that each vane only needed to span 1 metre of the 2 metre tunnel duct.

### 3.6. Straightening (Honeycomb) Section

The straightening or honeycomb section is a bank of tubes or cells aligned with the wind tunnel axis. All air must flow through one of these cells and thus any lateral momentum due to eddy motion in the airstream is absorbed. Wind tunnel design rules of thumb [9] state that the straightener cells should have a length at least 8 times their width. Cells must be small so that turbulence generated within the cell will be of a correspondingly small scale and thus be quickly dissipated by viscosity.

In horizontal wind tunnels the honeycomb can simply consist of drinking straws or some other such cylinder stacked from floor to ceiling within the tunnel. In a vertical tunnel, however, the honeycomb must be self-supporting under the weight of gravity. In the CSIRO wind tunnel we selected hollow-section polycarbonate roofing material manufactured in sheets of 2.4 m  $\times$  1.2 m and 10 mm thick. The hollow internal square section of this material is in the order of 8  $\times$  8 mm with  $\approx$ 1 mm walls. This material was cut into strips 2 m wide and 80 mm long and then stacked and glued until a 2 m  $\times$  2 m  $\times$  80 mm honeycomb was constructed.

The honeycomb section has an open space ratio of 80% (viz.  $b = 0.8$ ) and hence the coefficient  $k$  is 0.31. The pressure drop across the honeycomb, calculated using Equation 2, is a negligible 1.24 Pa. (This reasonably assumes that the resistance of the 80 mm long straightening tubes is comparable to that of a grid of the same open space ratio.)

## 4. Contractor Design

### 4.1. General

To this point in the wind tunnel the turbulent air from the fan has been slowed, screened to attenuate large-scale turbulence, turned, and passed through a honeycomb to straighten the air flow to further reduce large-scale turbulence. The air flow is now parallel with reasonable uniformity of the mean flow across the width of the tunnel. The final and most critical process in producing very uniform flow is the contraction of this air flow to speed it up to working velocities prior to entry to the working section.

The acceleration of the air flow should take place over as short a distance as possible for two reasons: 1) to minimise the build-up of the boundary layer (that layer of air slowed by friction due to the walls), and, in the case of vertical tunnels, 2) to keep the final height of the tunnel within reason (and planning guidelines). The distance, however, should not be so short that the air flow stalls on tight radius curves.

The contractor was designed using the formulations Borger [10] described in his extensive thesis on contractor optimisation. Borger's optimisation design requires that the curves of the contractor walls asymptote at both the inlet and outlet where both the first and second derivatives are zero. This ensures that at the inlet and outlet of the contractor there exists a stabilised parallel flow and an associated isobaric surface. If flow separation from the wall is successfully avoided, a flow uniformity within  $\pm 0.5\%$  will result.

### 4.2. Borger's Contractor Profile Curves

Borger developed an equation for a general function which commences at the origin of the XY plane with a specifiable derivative, i.e.  $y'_0$ . The curve then asymptotes to a specifiable point  $(x_w, y_w)$  where the first and second derivative conditions, i.e.  $y'_w = 0$  and  $y''_w = 0$ , will exist.

Two curves from this family (same  $y'_0$  but differing  $x_w, y_w$  pair) are spliced together after reflecting one of the curves once about each axis (Figure 3). The origin is subsequently known as the 'inflection point,'  $w_p$ , of the contractor profile. Borger then has a series of tabulations which, depending on the required contraction ratio, allow the designer to determine the precise values for the two sets of parameters  $(y'_0, x_w, y_w)$  giving the optimally short contractor profile.

The design of the CSIRO wind tunnel called for a contraction area ratio of 7.11:1, i.e. the cross-section of the contractor reduces from 2000 mm  $\times$  2000 mm at the inlet to 750 mm  $\times$  750 mm at the outlet to the working section. Borger gives a series of charts that specify parameters which describe the contractor proportions as a function of  $\eta_E$ , the square root of the inverse of the contractor ratio. In the case of the CSIRO tunnel,  $\eta_E = 0.375$ .

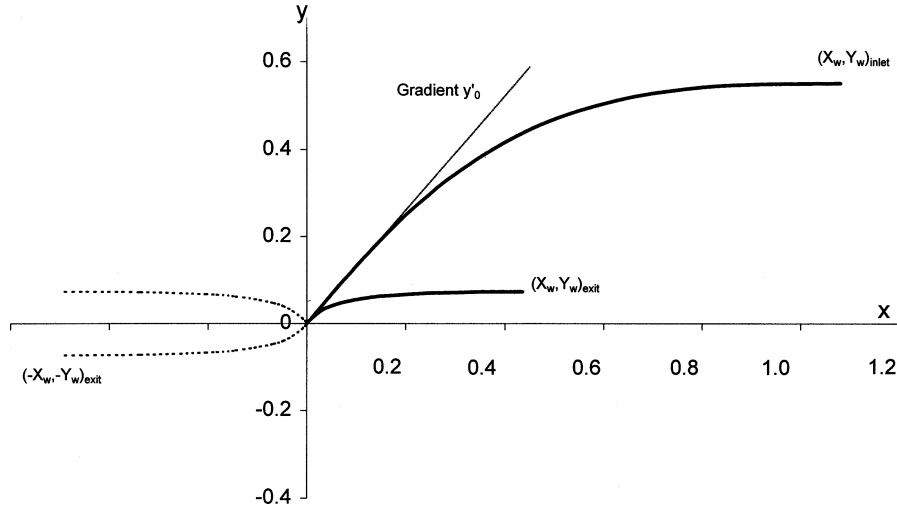


**Figure 3. Resultant curves for CSIRO wind tunnel obtained from Equations 4.1–4.4. Starting coordinates for the inlet and outlet curves  $(x_w, y_w)_{\text{inlet}}$  and  $(x_w, y_w)_{\text{exit}}$  are obtained from Borger's charts of contractor parameters as a function of  $\eta_E$ , the normalised half-width of the contractor exit. The common gradient,  $y'_0 = 1.348$ , is also obtained from values Borger gives as a function of  $\eta_E$ . The curve of  $(-x_w, -y_w)_{\text{exit}}$  has been mirrored around both axes.**

#### 4.3. Borger's Contractor Profile Equations

Borger [10, (p. 79)] gives a set of equations (Equations 4.1–4.4) to calculate the component curves that form the entrance and exit of the contractor based on the determined contractor parameters. For two sets of contractor parameters, two curves, one for the inlet side to the point of inflection,  $w_p$ , and one for the outlet side to  $w_p$ , are determined.

Equation 4.1 gives an intermediate variable,  $\bar{x}_w$ , that enables Equations 4.3 and 4.4 to be solved:

$$\bar{x}_w = \frac{15}{7} \left[ x_w - \frac{y_w}{y'_0} \right] \quad (4.1)$$

where  $x_w$ , and  $y_w$  are parameters given by Borger in charts as a function of  $\eta_E$ , and  $y'_0$  is the gradient of the family of curves given by the function:

$$y'_0 = \frac{w_s w_h}{w_l} \quad (4.2)$$

where  $w_s$ ,  $w_h$  and  $w_l$  are also parameters determined by Borger in charts as a function of  $\eta_E$ .

The value for  $\bar{x}_w$  is then substituted in Equation 4.3:

$$y = 3 \frac{y_w}{8\bar{x}_w^5} \bar{x}^5 - 5 \frac{y_w}{4\bar{x}_w^3} \bar{x}^3 + \frac{15y_w}{8\bar{x}_w} \quad (4.3)$$

to generate a series of points  $(\bar{x}, y)$ , where  $\bar{x}$  is a variable,  $0 \leq \bar{x} \leq \bar{x}_w$ . By choosing an appropriate interval value for a range of values of  $\bar{x}$ , within the range 0 to  $\bar{x}_w$ , Equation 4.3 results in a series of  $y$  values. These are then used to determine corresponding  $x$  values using Equation 4.4:

$$x = \bar{x} - y \left( \frac{8}{15} \frac{\bar{x}_w}{y_w} - \frac{1}{y'_0} \right) \quad (4.4)$$

The resultant coordinate pairs  $(x, y)$  give the curve of the contractor profile.

#### 4.4. CSIRO Wind Tunnel Values

In the case of the CSIRO wind tunnel, the contractor parameters were:

for the inlet curve:

$$x_w = 1.08 \text{ and } y_w = 0.552$$

for the exit curve:

$$x_w = 0.49 \text{ and } y_w = 0.073$$

The common gradient at the origin for both curves is

$$y'_0 = 1.348.$$

Figure 3 shows the resultant curves used in the CSIRO wind tunnel. The curve for the outlet part of the profile has been mirrored around both the  $x$  and  $y$  axes thus forming the complete profile of the contractor when joined with the curve for the inlet.

All the values hitherto used in Equations 4.1–4.4 have been dimensionless values, normalised by Borger to the proportions of the inlet. By coincidence, the proportions of the inlet of the CSIRO wind tunnel are such that the normalising factor is 1 (i.e. the half-width of our inlet is 1 m). Therefore all non-dimensional numbers can be viewed as being in the dimension of metres. Thus  $\eta_E$ , or the half-width of the exit, is 0.375 m and all values calculated for  $x$  and  $y$  can also be taken as in metres. If the proportions had not been so serendipitous, then the values calculated by Equations 4.3 and 4.4 would have to be scaled appropriately.



#### 4.5. CSIRO Wind Tunnel Contractor Shape

The curves generated by Equations 4.3 and 4.4 shown in Figure 3 are for axially-symmetric (i.e. circular cross-section) contractors. Being a square section contractor, the  $x$  axis must be stretched by 30% [10] to accommodate the fact that the profile of the contractor in the corners is longer than the profile in the centres of each side (Figure 4). Thus the CSIRO contractor has a length of  $1.57 \text{ m} \times 1.3 = 2.04 \text{ m}$ . Borger [10] also has formulated a refinement; a slight divergence at the exit of the contractor to compensate for boundary layer buildup which acts to constrict the outlet. This refinement was not incorporated into the CSIRO tunnel.

#### 4.6. Contractor Construction

A finite difference method was used to transform the  $x$  and  $y$  co-ordinate pairs into  $s$  and  $y$  co-ordinate pairs where  $s$  is the distance along the curve. This co-ordinate system then allowed the curves to be accurately cut from flat sheets of particle board such that they would form the correct profile once bent into shape on a purpose-built jig that matched the profile.

Particle board was selected for its uniform bending qualities. Each of the four sides was formed separately on this jig by laminating three 3 mm sheets of particle board.

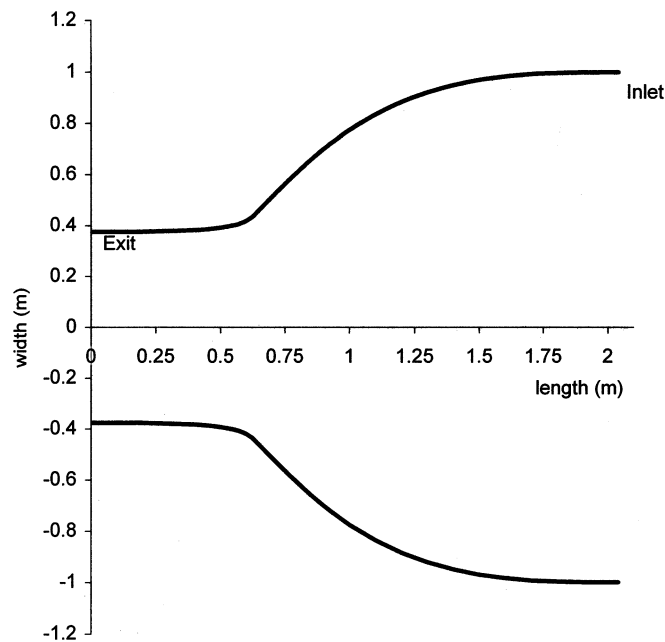


**Figure 4. The scaled, stretched ( $\times 30\%$ ) and joined curves that resulted for the profile of the CSIRO wind tunnel contractor. Two sides of the contractor profile are shown, mirrored around the centre-axis of the contractor. Note value of dimensionalised  $\eta_E$  as the half-width of the exit of the contractor.**

With three laminations the sides retained close to their design shape when removed from the jig.

The final correct shape was imposed once these sides were joined at the edges using the stitch and glue method. In this method the sides are stitched together with copper wire before strengthening the joints with glass-reinforced resin. This method is commonly used in dinghy construction and produces a strong, rigid contractor capable of supporting the weight of the working section.

## **5. Working Section**

### **5.1. Working Section Design**

The purpose of the tunnel is to observe embers as they burn at their terminal velocity. The initial terminal velocity must be estimated prior to the release of the ember and the terminal velocity will subsequently change as the ember is consumed. The working section was made with a divergent taper, from 750 mm at the entrance to 1.0 m over its length. The velocity at the top of this working section is approximately 56% of that at the bottom. (The speed at the top will in reality be slightly more than this geometrically-derived figure due to the constriction of air flow produced by the build-up of the boundary layer.)

This divergence provides a velocity gradient such that embers find their own terminal velocity without the need for critical fan speed adjustment. Bradshaw and Parkhurst [9] recommended that the total angle of divergence should not exceed 5° if separation of the boundary layer from the wall is to be avoided. At 4.25 metres in length the CSIRO tunnel has a working section divergence of 3.4°.

A small door in one wall of the working section allowed firebrands to be launched. Flyscreens on all windows ensured that the flaming embers could not escape.

### **5.2. Unmodified Flow**

In initial tests (unmodified flow) embers were found to strike the wall too frequently for useful observations to be made. The unmodified airflow into the working section was measured with a pitot tube and had a standard deviation in the mean air flow of 0.47%. At the exit to the tunnel the standard deviation from the mean flow was measured at 0.44% (excluding the boundary layer zone). See Knight *et al.* [6] for more detail on wind tunnel performance measurement techniques.

The boundary layer increased in thickness from 35 mm at a distance of 100 mm into the working section to 200 mm at a distance of 4.1 metres into the section (Figure 5). One side of the tunnel experienced significantly greater boundary layer growth and this was attributed to a mismatch in a joint between the contractor and working section of several mm. For the purpose of experiments carried out to date, it has not been necessary to correct this imperfection.

### **5.3. Modified Flow**

In order to reduce the frequency of embers striking the wall we needed to create a cross-stream velocity profile such that embers would be trapped in the centre of the working

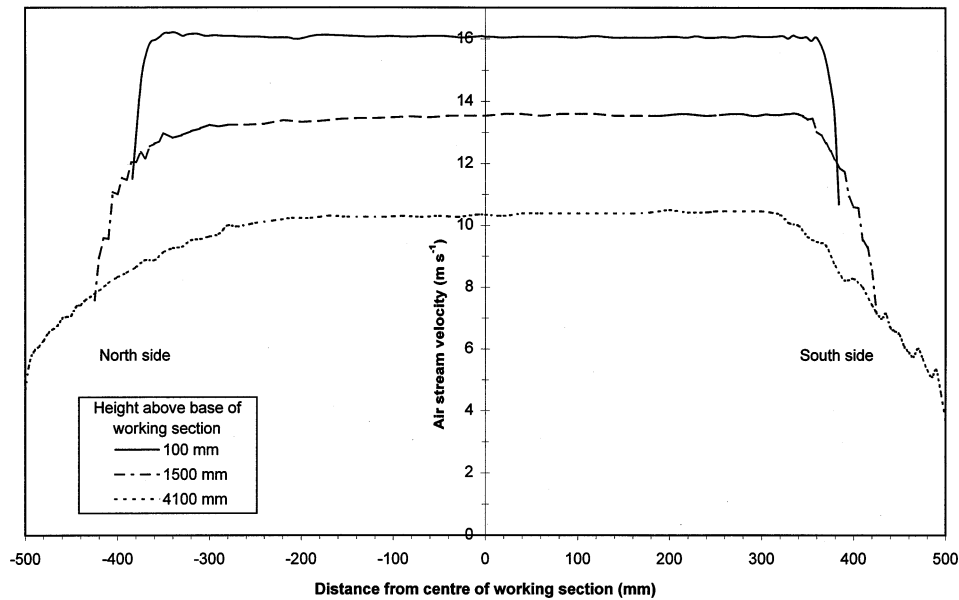


**Figure 5. Air stream velocity profiles for three heights (100 mm, 1500 mm, and 4100 mm) above base of working section. The increased build-up of the boundary layer on the north wall when compared to the south wall is evident.**

section. This was done by installing insect screens between the contractor outlet and entrance to the working section. The insect screens were laminated to produce a layer of varying thickness which resulted in an accelerated boundary layer and a reduced centre flow. The number of layers increased from 1 at the perimeter to 3 in the centre. Figure 6 shows the modified profile at 1000 mm height in the working section. The general form of this profile is maintained throughout the entire length of the working section. The speed of the low-speed central zone relative to the perimeter zone increases with height as a result of the positive pressure gradient forced by the divergent tunnel. The profile as shown effectively captures embers in the central zone.

## 6. Pressure Losses

Pressure varies in a wind tunnel according to the Bernoulli principle as it passes through faster and slower sections. These pressure changes are, however, restored as the duct returns to its former size. In calculating the back pressure load on the fan we are interested in pressure changes associated with energy loss (energy converted to heat via turbulent cascades).

The pressure losses from the two screens and the straightener are 22.9, 7.8 and 1.2 Pa respectively. In the unmodified configuration the other major contributor is the exit loss. In an open tunnel the energy of the exiting airstream is lost. Once free of the

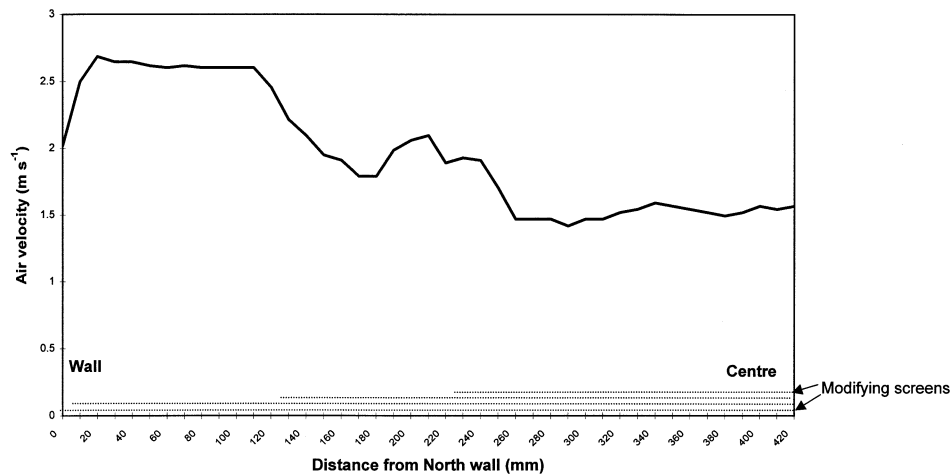


**Figure 6. The modified velocity profile at 1000 mm into the working section. Layout of modifying screens placed at the bottom of the working section is also shown. Distances to each edge of modifying screen is shown as from the wall. Due to the taper in the working section, the distance from the wall to the centre has increased and is not to scale. The variation in the air velocity around the edges of the modifying screens are a result of the build-up of the boundary layer at each edge.**

tunnel walls, turbulence sets in and the kinetic energy is converted to heat. At an exit speed,  $v$ , of  $10 \text{ m s}^{-1}$  where the tunnel cross-section,  $A$ , is  $1 \text{ m}^2$ , the lost power is  $1/2 A \rho v^3 = 635 \text{ watts}$ , where  $\rho$  is the density of air ( $1.27 \text{ kg m}^{-3}$ ). This is equivalent to a pressure  $\times$  volume delivery of the fan. At a delivery rate of  $10 \text{ m}^3 \text{ s}^{-1}$  the exit loss pressure component required of the fan is thus  $63.5 \text{ Pa}$ —the fan's exit area also being approximately  $1 \text{ m}^2$ . Frictional losses at the walls are small enough to be neglected when estimating fan requirements. In our design we allowed for a maximum operating pressure drop across the fan (and hence across the whole tunnel) of  $300 \text{ Pa}$ . This was to allow for the resistance of the screens used to modify the airflow and scope for the fan to be run at higher than the  $10 \text{ m}^3 \text{ s}^{-1}$  used in our example calculations.

## 7. Discussion

The CSIRO wind tunnel has been a successful tool for the study of firebrands in flight. The design has proven to be both effective and economic in materials and construction. The unmodified airflow is uniform to within  $0.5\%$  [6].

The tunnel exhibited low frequency vibrations which were attributed to resonance of panels in the diffuser, turning section and working section, and the length of the tunnel. All these panels were constructed from  $12 \text{ mm}$  thick plywood and sections of  $1.2 \text{ m} \times 2 \text{ m}$  are currently unbraced. External bracing could easily be attached and should remove most of this vibration.

Mismatches of a few millimeters in the joins of the contractor to the working section were most likely responsible for accelerated boundary layer growth on one wall. As timber and plywood are a difficult material to work with to millimeter accuracy, we suggest fabricating sections in pairs, using the previous completed component as a jig for the following stage.

The divergent taper working section, at  $3.4^\circ$  total angle, did not suffer from boundary layer separation and yet was sufficient for practical observation of burning embers.

The method of accelerating the boundary layer with variable resistance screens, although primitive, was effective. Alternatives which may provide sharper boundaries between the high and low speed zones could be devised but would require the complexity of two separately controllable air sources.

Turning sections will inevitably introduce turbulence of the scale of the vane spacing (140 mm) and they are normally placed well upstream from critical sections to allow this turbulence to dissipate. The placing of the straightener and contractor a short distance from the turning section did not, however, have a great adverse affect on the quality of air flow.

Construction difficulties increase “exponentially” with size. Calculations following the kinetic energy increases of individual air parcels show that a 7.1:1 contractor will reduce a 20% variation in input flow to 0.5% at the contractor exit. If the widest cross-section was reduced from 2 metres to 1.5 metres, a 4:1 contraction could be used. A 4:1 contraction will reduce a 20% variation to 1.1% which is most probably adequate for firebrand studies. Similar porosity screens would be needed in the diffuser sections but note that a smaller cross-section will generate higher back pressures. Fans of the type selected, however, have a generous reserve of pressure capability and this should not be a problem. In fact enough pressure capability is in reserve to permit constructors to increase the number of screens to improve the flow quality into the contractor and so compensate for a lower contraction ratio.

The above suggestion maintains the working section with a 750 mm entrance. This is a practical size and we would not recommend making it smaller. Boundary layers will build up at the same rate regardless of tunnel width. That is, the boundary layer would encroach on a small tunnel producing an unworkably small centre zone a shorter distance into the working section.

Whilst the tapered working section allows a burning ember to fluctuate over a significant range of terminal velocities, there is a constant need to manually adjust the overall air flow velocity by altering the speed of the fan in order to keep the ember in a practical viewing “window.” While the speed of the fan responds quickly to the speed controller, human reaction times and hand/eye coordination while observing the ember’s flight are the limiting factors in the operational use of the wind tunnel. It was found that a good percentage of the 4.25 metre tapered working section length is needed to steady an ember and keep it captive.

If the tunnel is not hermetically sealed from ambient conditions fluctuations in measured velocity will occur during windy periods. This presents a difficulty in calibration, especially at low tunnel speeds. Calibration thus involved repeated measurements on the quieter days, so that fluctuations could be removed statistically. See Ellis [5] for a full description of calibration techniques.

## 8. Acknowledgements

Funding to investigate the phenomena of spotting in Australian forests and build the CSIRO vertical wind tunnel was kindly made available by the Mayne Nickless Corporation. The author wishes to thank the members of the CSIRO Forestry and Forest Products Bushfire Behaviour and Management Group who assisted in the construction of the facility, and especially Ricky Jordan who provided invaluable carpentry skills.

## References

- [1] C.S. Tarifa, P.P. del Notario, and F.G. Moreno, "On the Flight Paths and Lifetimes of Burning Particles of Wood," Proceedings of Tenth Symposium (International) on Combustion, 1965, pp. 1021–1037.
- [2] C.S. Tarifa, P.P. del Notario, F.G. Moreno, and A.R. Villa, "Transport and Combustion of Firebrands," Final Report of Grants FG-SP-114 and FG-SP-146, Aeronautical Institute of Madrid, 1967, 90 pp.
- [3] A. Muraszew, J.B. Fedele, and W.C. Kuby, "Firebrand Investigation," Aerospace Report No. ATR-75(7470)-1, Vehicle Engineering Division, The Aerospace Corporation, El Segundo, CA, 1975, 104 pp.
- [4] A. Muraszew, J.B. Fedele, and W.C. Kuby, "Investigation of Fire Whirls and Firebrands," Aerospace Report No. ATR-76(7509)-1, Vehicle Engineering Division, The Aerospace Corporation, El Segundo, CA, 1976, 155 pp.
- [5] P.F. Ellis, "The Aerodynamic and Combustion Characteristics of Eucalypt Bark—A Firebrand Study," Ph.D. thesis, Australian National University, Canberra, 2000, 187 pp.
- [6] I.K. Knight, P.F. Ellis, and A.L. Sullivan, "A Vertical Wind Tunnel for Investigating the Combustion Behaviour of Firebrands at Their Terminal Velocity," CSIRO Forestry and Forest Products Technical Report No. 133, Canberra, Australia.
- [7] Fantech Pty Ltd., *Fans by Fantech: A Manual of Selection Data and Recommended Practice*. Melbourne, Australia: The Craftsman Press, 1993, unpaginated.
- [8] R.D. Mentah, "Aspects of the Design and Performance of Blower Tunnel Components," Ph.D. thesis, London University, Boston Spa, England, 1994.
- [9] P. Bradshaw, and R.C. Parkhurst, "The Design of Low Speed Wind Tunnels," Aero Report 1039, National Physical Laboratory, Teddington, England, 1962, 64 pp.
- [10] G.G. Borger, "The Optimisation of Wind Tunnel Contractions for the Subsonic Range," Ph.D. thesis, Ruhr University, 1973. [NASA (English) Translation TT-F-16899, NASA, Washington DC, 1976, 188 pp.]